

## Study of $\text{Cu}_2\text{ZnSn}(\text{S,Se})_4$ Thin Films for Solar Cell Application

Muhammad Monirul Islam<sup>1,2,\*</sup>, Mohammad Abdul Halim<sup>2</sup>, Chon Joy<sup>2</sup>, Xianjia Luo<sup>2</sup>, Takeaki Sakurai<sup>2</sup>, Noriyuki Sakai<sup>3</sup>, Takuya Kato<sup>3</sup>, Hiroki Sugimoto<sup>3</sup>, Hitoshi Tampo<sup>4</sup>, Hajime Shibata<sup>4</sup>, Shigeru Niki<sup>4</sup>, Akimoto Katsuhiko<sup>1,2</sup>

<sup>1</sup>Graduate School of Pure and Applied Sciences, Alliance for Research on North Africa (ARENA), University of Tsukuba, Japan.

<sup>2</sup>Institute of Applied Physics, University of Tsukuba, Japan.

<sup>3</sup>Energy Solution Business Center, Showa Shell Sekiyu K.K., Japan.

<sup>4</sup>National Institute of Advanced Industrial Science and Technology (AIST), Japan.

E-mail: islam.monir.ke@u.tsukuba.ac.jp

**Abstract.**  $\text{Cu}_2\text{ZnSn}(\text{S,Se})_4$  (CZTSSe) thin films with various Cu/Sn ratio in the films have been investigated to study the effect of compositional variation over the electrical, optical, and structural properties of the film. Surface morphology and grain size were found to be significantly influenced by the Cu/Sn ratio in the films and grain size was found better for the samples with moderate Cu/Sn ratio of 1.75. Irrespective of the growth condition and compositional variation, all the CZTSSe crystals show that grains are oriented along (112) direction as evident from the room temperature XRD data. Dark current-voltage (*I-V*) curve reveals that that sample with Cu/Sn = 1.75 exhibits lowest leakage current, while sample with Cu/Sn = 1.85 has the highest leakage current along with larger ideality factor indicating larger recombination centers in this film. Series resistance was also found to be higher in the sample with higher Cu-content. An anomaly in the optical band-gap has been explained with the presences of impurity phases and compositional inhomogeneities in the CZTSSe materials.

### 1. Introduction

In order to fulfil the global increasing energy-demand using technologies which are compatible with the realization of green environment, recently various alternative sources of electricity have been emerged including photovoltaic (PV) technology; more specifically solar cells. Immediate challenge of the PV technology is the cost of electricity generation. Therefore, research and development of solar cells with earth-abundant non-toxic absorber material along with low production cost should be of highly prioritized. Quaternary compound  $\text{Cu}_2\text{ZnSn}(\text{S,Se})_4$  (CZTSSe) is a promising material for absorber layer in the solar cells [1-3]. CZTSSe utilizes Zn and Sn in replacement of scarce material, Ga and In in the  $\text{Cu}(\text{In,Ga})\text{Se}_2$ . Thus, CZTSSe becomes a potential alternative to chalcogenide-based thin film solar cells including  $\text{Cu}(\text{In,Ga})\text{Se}_2$  and CdTe mainly because of abundance and non-toxicity of the constituent elements. Band gap of the  $\text{Cu}_2\text{ZnSnSe}_4$  is 1.04 eV [4], while it becomes 1.5 eV [5] for its  $\text{Cu}_2\text{ZnSnS}_4$  counterpart. Thus, band-gap of the  $\text{Cu}_2\text{ZnSn}(\text{S,Se})_4$  can be controlled by varying the Se/S ratio in the material. In case of the single junction solar cell, the ideal band-gap of the absorber layer to achieve the highest conversion efficiency under AM 1.5 sunlight is speculated



theoretically to be around 1.4 eV [6]. However, laboratory-scale efficiency of  $\text{Cu}_2\text{ZnSn}(\text{S},\text{Se})_4$  solar cell so far has been reported as high as ~12 % [7], while pure  $\text{Cu}_2\text{ZnSnS}_4$  shows efficiency around 8 % [8]. Moreover, efficiency is still behind the  $\text{Cu}(\text{In},\text{Ga})\text{Se}_2$  counterpart which is around 21 % [9]. A complete understanding of the growth mechanism, growth condition and their correlation with the material properties, and their impact over the device performances must be the key issue to achieve efficiency beyond the current limit. The electrical, optical and micro-structural properties of the CZTSSe films are dominated by the various intrinsic defects originated from the off stoichiometry of the film composition. Moreover, deviation from the ideal stoichiometry during growth of this material might produce several secondary phases that includes,  $\text{Zn}(\text{S},\text{Se})$ ,  $\text{Sn}(\text{S},\text{Se})$ ,  $\text{Cu}_2(\text{S},\text{Se})$ ,  $\text{Cu}_2\text{Sn}(\text{S},\text{Se})_3$  etc. [10,11]. Therefore, to achieve the optimized material quality of the CZTSSe material, an extensive study of this material with various compositions is indispensable. In this paper, we have systematically varied the Cu/Sn CZTSSe absorber-layer to study the effect of compositional variation on the electrical, optical, and structural properties of the film.

## 2. Experimental

Polycrystalline CZTSSe thin films with typical thickness of 1.25  $\mu\text{m}$  were grown over Mo coated sodalime glass (SLG) substrates using sulfo-selenization process. Samples were grown by Energy Solution Business Center, Showa Shell Sekiyu KK, Japan. Several CZTSSe samples with various Cu/Sn ratios in the film were prepared to study the effect of compositional variation, more specifically Cu-content on the films. Cu/Sn ratio in the films is determined based on the starting material precursor. S/Se ratio in all the samples is kept constant. Solar cell structure is consisted of  $n\text{-ZnO}/i\text{-ZnO}/\text{CdS}/\text{Cu}_2\text{ZnSn}(\text{S},\text{Se})_4/\text{Mo}/\text{SLG}$ . The composition of the grown CZTSSe films was measured by electron probe micro-analysis (EPMA) at 15 kV of acceleration voltage. The structural properties of the films were examined by scanning electron microscopy (SEM). X-Ray diffraction (XRD) was taken in the range of  $15^\circ\sim 90^\circ$  by philips X'pert diffractometer at  $\theta\text{-}2\theta$  mode with  $\text{Cu-K}\alpha$  ( $\lambda = 1.541837 \text{ \AA}$ ) radiation operated at 40 kV and 30 mA. Electrical properties were studied by the measuring the current-voltage ( $I\text{-}V$ ) at dark using solar simulator. Optical band-gap was analyzed from the investigation of the external quantum efficiency (EQE) measurement of the solar cell structure. All characterizations were performed at room temperature.

## 3. Results and Discussion

### 3.1. Structural properties

For the study of the structural properties of the CZTSSe thin films, sample structure was considered as CZTSSe/Mo/SLG. Shown in figure 1(a)-(c) are the SEM images of the surface view of the several CZTSSe thin films grown with various Cu/Sn ratios in the films.

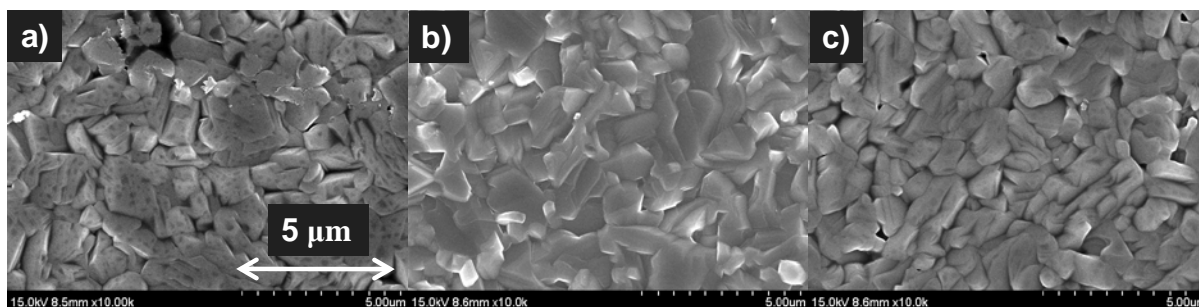


**Figure 1.** SEM images of the surface view of the several CZTSSe samples grown with a) Cu/Sn = 1.65, b) Cu/Sn = 1.75, and c) Cu/Sn = 1.85.

From the surface view, it is apparent that Cu-content in the films influences the morphology and the structure of the film including the grain size and shape. Film with Cu/Sn = 1.75 shows the morphology with large and uniform grains as seen from the Figure 1(b). No void or impurity phases were seen on the surface of the film. With decreasing the Cu-content in the film with Cu/Sn = 1.65 (Figure 1(a)), no apparent reduction in the grain size was observed. However, overall morphology deteriorates. There are some voids appeared inside grains. With a increase of the Cu-content (Cu/Sn = 1.85) grains become smaller in size with increasing number of voids inside grain boundaries. The shape also tends to be little granular for this sample. Smaller grains and voids strongly influence electrical properties of the polycrystalline material. Grain boundary act as scattering and recombination center for free carriers in the semiconductor. Thus increased grain-boundary increases the resistivity and reduces free carrier concentration of the material [12].

Shown in figure 2 is the XRD data for several CSTSSe films taken in the range of  $2\theta = 10^\circ$  to  $90^\circ$ . XRD was taken on the structure of CIGS/Mo/SLG. No apparent differences have been observed in the XRD data for several samples with different Cu/Sn ratio in the film. The presence of (002) and (101) peak suggest that crystal structure of the films is either kesterite or stannite-type [13]. All the samples show well resolved (112) peak which is larger in intensities than the (220)/(204) peak. It indicates that irrespective of the growth condition, grains of the CSTSSe crystals find (112) orientation as kinetically preferable and grains continue to develop along this direction. Since the major diffraction peaks of CZTSSe overlaps with those of  $\text{Cu}_2\text{Sn}(\text{S},\text{Se})_3$ ,  $\text{Cu}_2(\text{S},\text{Se})$  and  $\text{Zn}(\text{S},\text{Se})$  phases, it is difficult to distinguish those phases from the CZTSSe phase in the XRD data. However, quantitative phase analysis of the rietveld refinement of XRD data of a separate CZTSSe sample (not shown here) reveals that significant amount of  $\text{Cu}_2(\text{S},\text{Se})$  and  $\text{Sn}(\text{S},\text{Se})$  co exist with the CZTSSe phase.

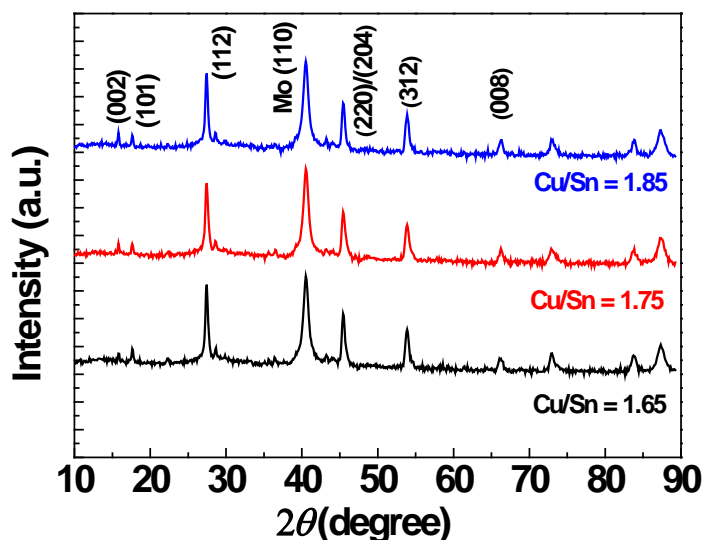


**Figure 2.** XRD data of several CZTSSe samples grown with a) Cu/Sn = 1.65, b) Cu/Sn = 1.75, and c) Cu/Sn = 1.85

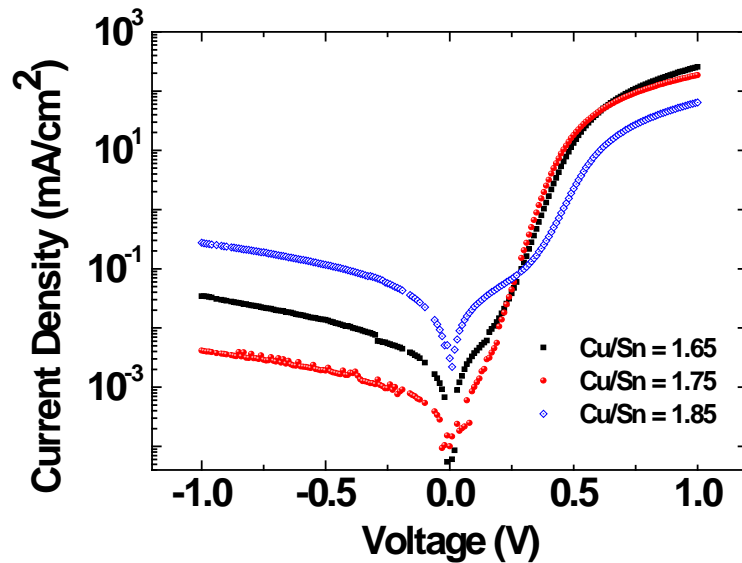


**Figure 3.** Dark  $I$ - $V$  curve of the fabricated CZTSSe based solar cells where CZTSSe absorber-layers were grown with various Cu/Sn ratios in the film.

### 3.2. Electrical properties

Electrical properties of the CZTSSe samples were investigated by measuring the dark  $I$ - $V$  curve of the solar cell structures.  $I$ - $V$  curve of a  $p$ - $n$  junction solar cell can be presented using single diode model as follows [14]:

$$J = J_0 \exp \left[ \frac{q}{nkT} (V - RJ) \right] + G(V - RJ) - J_L \quad (1)$$

Here,  $J$  is the diode current density,  $J_0$  denotes the saturation current density,  $q$  is the elemental charge,  $n$  is the diode ideality factor,  $k$  denotes the Boltzmann constant,  $T$  is the temperature,  $V$  is the applied voltage,  $R$  is the series resistance,  $G$  is the shunt conductance, and  $J_L$  is the photo current density. For the measurement at the dark, we can consider  $J_L = 0$ . In the forward bias region, the equation can be simplified as:

$$J = J_0 \exp \left[ \frac{q}{nkT} (V - RJ) \right] \quad (2)$$

Then, ideality factor and saturation current density at a particular temperature can be determined from the slope of the  $\ln(J)$ - $V$  curve. Figure 3 shows the dark  $I$ - $V$  curve of all the solar cell structures fabricated with CZTSSe absorber layer. Flatten of the curves after  $V \sim 0.5$  volt is due to effect of series resistance. It is apparent from the figure that sample with Cu/Sn = 1.75 exhibits lowest leakage current, while sample with Cu/Sn = 1.85 has the highest leakage current. Table-1 lists extracted diode ideality factor and saturation current density for all the samples. Series resistance was also calculated and listed in the table.

**Table 4.** Electrical parameters of the CZTSSe Solar cells extracted from the fitting of the dark  $I$ - $V$  curve.

Cu/Sn	Ideality factor (n)	Saturation current density, $J_0$ (mA/cm <sup>2</sup> )	Series Resistance ( $\Omega$ -cm <sup>2</sup> )
<b>1.65</b>	1.64	$1 \times 10^{-4}$	1.7
<b>1.75</b>	1.38	$4 \times 10^{-5}$	2.2
<b>1.85</b>	2.25	$4 \times 10^{-4}$	5.4

As seen from the table, all the samples show relatively higher ideality factor. It suggests that the performance of the solar cells is controlled by the recombination through localized states in the depletion region of the absorber layer. In particular, ideality factor of 2.25 together with higher leakage current of  $4 \times 10^{-4}$  mA/cm<sup>2</sup> and higher series resistance in case of the sample with Cu/Sn = 1.85 indicate that current transport properties of this sample is also dominated by recombination at the interface as well as recombination through trap assisted tunnelling. Higher series resistance also affect fill factor and current density of the solar cells.

### 3.3. Optical Properties

Optical band-gap of the CZTSSe materials has been determined from the measurement of the external quantum efficiency ( $QE$ ) of the completed device. Assuming that all the carriers generated in the depletion region,  $W$  are collected without recombination loss and those generated within the diffusion length,  $L$  in the neutral region diffuse to the depletion edge,  $QE$  of the CZTSSe based solar cell can be approximated as [15]

$$QE(h\nu) = 1 - \frac{\exp[-\alpha(h\nu)W(V)]}{\alpha(h\nu)L+1} \quad (3)$$

Where,  $\alpha(h\nu)$  is the absorption coefficient,  $h\nu$  is the energy, and  $V$  is the bias voltage. At a particular bias voltage, assuming  $\alpha(h\nu)L \ll 1$ , the above equation can be more simplified as

$$QE(h\nu) \sim 1 - \exp[-\alpha(h\nu)W] \quad (4)$$

$$\alpha(h\nu) \sim -\ln(1 - QE(h\nu)) \quad (5)$$

Thus,  $QE$  in the sub-band gap region is proportional to the optical absorption coefficient of the material. Since, the optical band-gap is related to the photon energy near the band edge through the relationship [16],

$$\alpha h\nu \sim (h\nu - E_g)^{1/2} \quad (6)$$

Thus, it is possible to estimate the band-gap,  $E_g$  from the long wavelength tail of the  $QE$  plot against the incident photon energy,  $E$ . Shown in figure 4 is the optical band-gap of CZTSSe films grown with different Cu/Sn ratio in the films. From the figure it has been seen that optical band-gap of all the three samples is around 1.06 eV. A small difference is apparent among the band-gap of the films. sample with Cu/Sn = 1.85 shows relatively smaller band-gap. As mentioned earlier, it has been reported that chalcopyrite CZTSSe films contains several impurity phases which may include  $Cu_2Sn(S,Se)_3$ ,  $Cu_2(S,Se)$ ,  $Zn(S,Se)$ ,  $Sn(S,Se)_2$ ,  $Cu_4Sn(S,Se)_4$  etc. Of course the existence of impurity phases depends on the growth condition and growth technique of the CZTSSe material. Nevertheless, electrical and optical properties of the CZTSSe material are determined by those impurity phases

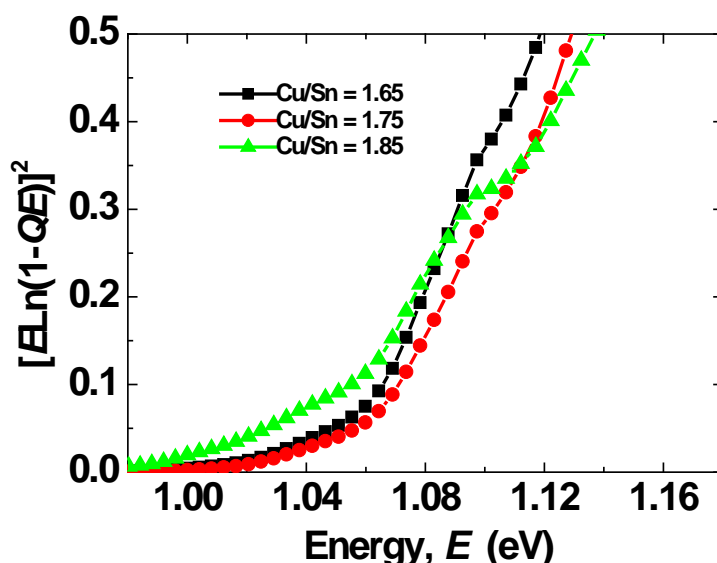


**Figure 4.** Optical band-gap energy of the CZTSSe thin films, determined from the long wavelength tail of the  $QE$  curve of the complete solar cell.

included in the material. For example, carrier concentration and optical band-gap of the CZTSSe material depend on the conduction-type and band-gap of the impurity phases. From the EPMA data it has been seen that for the samples with Cu/Sn ratio of 1.65, 1.75, and 1.85, Zn/Cu ratio are 0.58, 0.56, and 0.53 respectively. Therefore, Zn-rich phase is possible to be formed in the sample with Cu/Sn = 1.65, while Cu-rich phase may be formed in the sample with Cu/Sn = 1.85. Therefore, there might be some anomalies in the band-gap of the CZTSSe films arising from those impurity phases. Moreover, it can be seen from the figure 4 that there is band-gaps gradient in all the samples which suggests compositional inhomogeneities in all the CZTSSe samples.

#### 4. Conclusions

CZTSSe thin films with various Cu/Sn ratio in the films have been investigated to study the effect of compositional variation over the electrical, optical, and structural properties of the film. It has been seen that surface morphology and grain size are significantly influenced by the Cu/Sn ratio in the films and morphology was found better for the samples with moderate Cu/Sn ratio of 1.75. Irrespective of the growth condition and compositional variation, all the CZTSSe crystals show (112) orientation as evident from the room temperature XRD data. In consistent with the SEM data, dark  $I$ - $V$  curve reveals that that sample with Cu/Sn = 1.75 exhibits lowest leakage current, while sample with Cu/Sn = 1.85 has the highest leakage current along with larger ideality factor indicating larger recombination centers in this film. An anomaly in the optical band-gap has been explained with the presences of impurity phases and compositional inhomogeneities in the CZTSSe materials.

#### 5. Acknowledgments

This work is performed under the program supported by the New Energy and Industrial Technology Development organization (NEDO) and the Ministry of Economy, Trade and Industry (METI), Japan.

## References

- [1] Tanaka T, Nagatomo T, Kawasaki D, Nishio M, Guo Q, Wakahara A, Yoshida A and Ogawa H 2005 *J. Phys. Chem. Sol.* **66** 1978
- [2] Katagiri H, Jimbo K, Yamada S, Kamimura T, Maw W S, Fukano T, Ito T and Motohiro T 2008 *Appl. Phys. Express* **1** 041201
- [3] Scragg J J, Berg D M and Dale P J 2010 *J. Electroanal. Chem.* **646** 52
- [4] Chen S, Gong X G, Walsh A and Wei S -H 2009 *Appl. Phys. Lett.* **94** 041903
- [5] Perrson C 2010 *J. Appl. Phys.* **107** 053710
- [6] Shockley W, Queisser H 1961 *J. Appl. Phys.* **32**, 510
- [7] Wang W, Winkler M T, Gunawan O, Gokmen T, Todorov T K, Zhu Y and Mitzi D B 2013 *Adv. Energy Mater.* **4** 1301465
- [8] Shin B, Gunawan O, Zhu Y, Bojarczuk N A, Jay Chey S and Guha S 2013 *Prog. Photovolt: Res. Appl.* **21** 72
- [9] Jackson P, Hariskos D, Lotter E, Paetel S, Wuerz R, Menner R, Wischmann W and Powalla M 2011 *Prog. Photovolt: Res. Appl.* **19** 894
- [10] Dudchak I and Piskach L 2003 *J. Alloys Compd.* **351** 145
- [11] Nagoya A, Asahi R, Wahl R and Kresse G 2010 *Phys. Rev. B* **81** 113202
- [12] Kazmerski L L, Berry W B and Allen C W 1972 *J. Appl. Phys.* **43** 3515
- [13] Xianzhong Lin, Jaison Kavalakkatt, Kai Kornhuber, Daniel Abou-Ras, Susan Schorr, Martha Ch. Lux-Steiner and Ahmed Ennaoui 2012 *RSC Advances* **2** 9894
- [14] Sze S M 1969 *Physics of Semiconductor Devices* (New York: Wiley-Interscience)
- [15] Liu X X and Sites J R 1994 *J. Appl. Phys.* **75** 577
- [16] Pankove Jacques I 1971 *Optical Process in Semiconductors* (New York: Dover)